Density Functional Theoretical Modeling, Electrostatic Surface Potential and Surface Enhanced Raman Spectroscopic Studies on Biosynthesized Silver Nanoparticles: Observation of 400...

ARTICLE *in* THE JOURNAL OF PHYSICAL CHEMISTRY A · MARCH 2014

Impact Factor: 2.69 · DOI: 10.1021/jp4090266 · Source: PubMed

6 AUTHORS, INCLUDING:

Sanchita Sil
Indian Institute of Science
19 PUBLICATIONS **24** CITATIONS
SEE PROFILE

Deepika Chaturvedi
Indian Institute of Science
18 PUBLICATIONS **84** CITATIONS
SEE PROFILE

Srividya Kumar
Indian Institute of Science
7 PUBLICATIONS **31** CITATIONS
SEE PROFILE

Siva Umapathy
Indian Institute of Science
143 PUBLICATIONS **1,434** CITATIONS
SEE PROFILE

THE JOURNAL OF PHYSICAL CHEMISTRY A

Article

pubs.acs.org/JPCA

Density Functional Theoretical Modeling, Electrostatic Surface Potential and Surface Enhanced Raman Spectroscopic Studies on Biosynthesized Silver Nanoparticles: Observation of 400 pM Sensitivity to Explosives

Sanchita Sil,[†,‡] Deepika Chaturvedi,[†] Keerthi B. Krishnappa,[†] Srividya Kumar,[†] S. N. Asthana,[‡] and Siva Umapathy[†,§,*]

[†]Department of Inorganic & Physical Chemistry Indian Institute of Science, Bangalore 560012, India

[‡]High Energy Materials Research Laboratory, Sutarwadi, Pune 411021, India

[§]Department of Instrumentation and Applied Physics, Indian Institute of Science, Bangalore-560012, India

Supporting Information

ABSTRACT: Interaction of adsorbate on charged surfaces, orientation of the analyte on the surface, and surface enhancement aspects have been studied. These aspects have been explored in details to explain the surface-enhanced Raman spectroscopic (SERS) spectra of 2,4,6,8,10,12-hexanitro-2,4,6,8,10,12-hexaazaisowurtzitane (HNIW or CL-20), a well-known explosive, and 2,4,6-trinitrotoluene (TNT) using one-pot synthesis of silver nanoparticles via biosynthetic route using natural precursor extracts of clove and pepper. The biosynthesized silver nanoparticles (bio Ag Nps) have been characterized using UV−vis spectroscopy, scanning electron microscopy and atomic force microscopy. SERS studies conducted using bio Ag Nps on different water insoluble analytes, such as CL-20 and TNT, lead to SERS signals at concentration levels of 400 pM. The experimental findings have been corroborated with density functional computational results, electrostatic surface potential calculations, Fukui functions and ζ potential measurements.

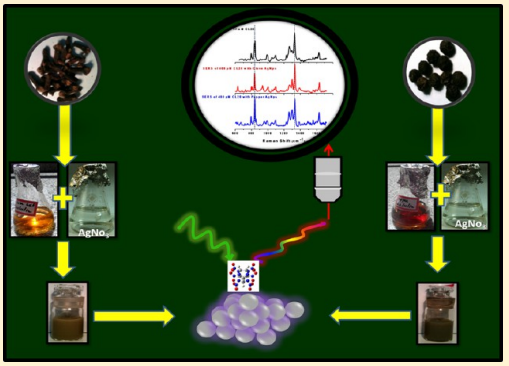

INTRODUCTION

Raman spectroscopy has been an important analytical tool for several decades now for the identification of molecular structures owing to its molecular specificity and the ease of sampling. However, due to the inherent weak nature of the Raman process, the detection of Raman scattered photons has been very challenging. This problem has been overcome by the discovery of enhanced Raman intensities on an Ag surface by Fleishmann et al. in 1974.[1] The confluence of Raman spectroscopy and Ag nanoparticles overcame the inherent drawback of the weaker signals and resulted in surface enhanced Raman spectroscopy (SERS).[2,3] The main advantage of SERS is the enhancement on the order of 10^5−10^6 of the Raman signal of an analyte when it is adsorbed to or near to the surface of certain noble metal structures with nanoscale features.[2−8] The Raman intensity enhancement leads to the detection of even single molecule.[9−12] Renaissance in the field of SERS was brought about in the past couple of decades by the rapid development of spectroscopic instrumentation, nano-fabrication techniques, novel detection schemes and theoretical modeling. This technique has also been applied for the trace detection of dyes, biological materials and nuclear wastes to name a few.[13−17]

Detection of explosives in trace quantities is one of the major challenges for the researchers around the globe for security and forensic applications. In addition, analysis of post blast residues, detection of unexploded ordnances as well as demining, adds to the problem of detection. SERS on dinitrotoluene (DNT), TNT, 1,3,5-trinitro-1,3,5-triazacyclohexane (RDX), pentaerytrhitol tetranitrate (PETN), nitroglycerine (NG), and triacetone triperoxide (TATP) has previously been reported.[18−25] In the present investigation, surface enhanced Raman spectroscopic technique has been employed to detect Rhodamine B (Rh B) (Figure 1a), TNT (Figure 1b), and CL-20 (Figure 1c) molecules using biosynthesized silver nanoparticles (Ag Nps) prepared using clove and pepper extracts as reducing agents.

Nanoparticles prepared using the biosynthetic routes are easy to prepare, cost-effective and eco-friendly and found to be reasonably stable over a period of time. CL-20, short form for China Lake, the place of its origin where it was synthesized by Nielsen et al. in 1986,[26] is regarded as the most powerful explosive with a very high velocity of detonation ∼9400 m/s. The cage like structure and six N-NO_2 moieties renders this

Received: September 9, 2013
Revised: March 20, 2014

   dx.doi.org/10.1021/jp4090266 | J. Phys. Chem. A XXXX, XXX, XXX−XXX

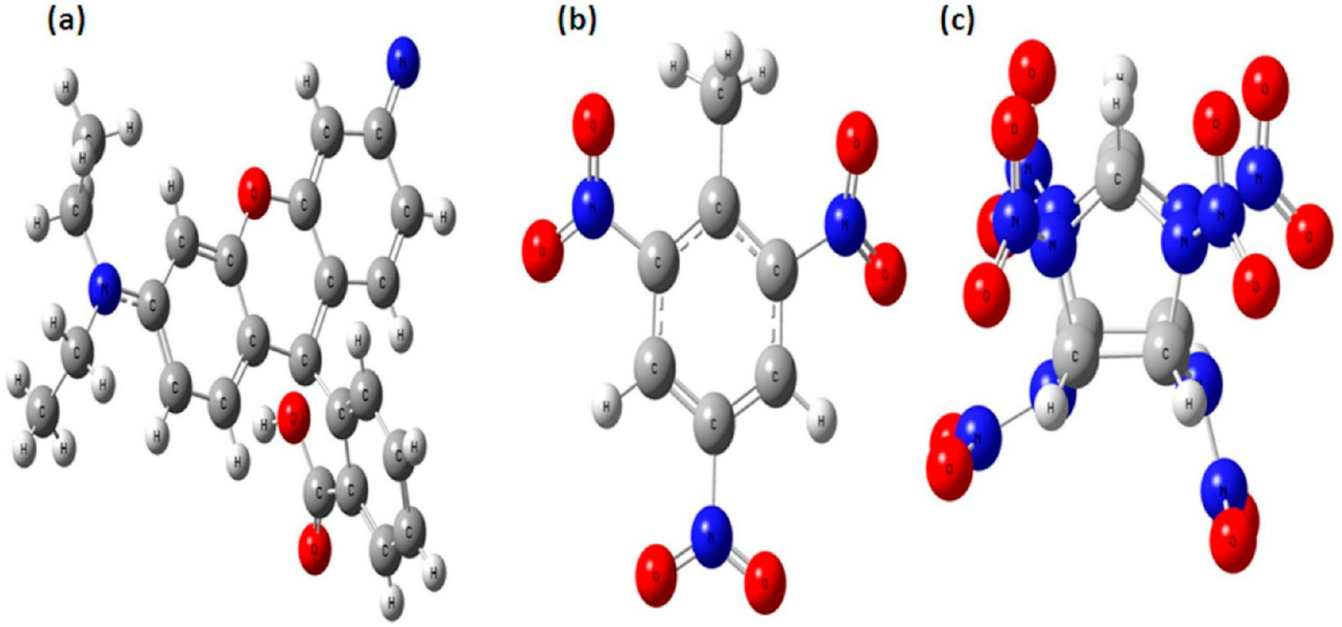

Figure 1. Structure of (a) Rh B (b) TNT and (c) CL-20.

molecule rich in energy.[27,28] Reports on single molecule detection of xanthene class of dye, Rhodamine 6G has been reported,[10,11] and TNT has been detected up to the tens of picogram level.[25] In this paper, the observation of the enhanced Raman signal for as low as 400 pM concentration of Rh B, TNT, and CL-20 using the bio Ag Nps is presented.

EXPERIMENTAL METHODS

Chemicals. Silver nitrate ($AgNO_3$), HPLC grade acetonitrile, and Rhodamine B were procured from S D Fine Chemicals. Clove and pepper were purchased from a local market. TNT and CL-20 were obtained from the High Energy Materials Research Laboratory, in Pune, India. Both TNT and CL-20 solutions were prepared in acetonitrile while the rest of the solutions were prepared using Millipore water (Bio cell Laboratories, Inc., Quantum EX).

Instrumentation. Surface Plasmon absorption spectra for the bio Ag Nps were recorded using a Perkin-Elmer UV−vis−NIR Spectrophotometer, model Lambda 750 series, in the visible wavelength range 200−800 nm. Scanning Electron Microscopic (SEM) studies of the bio Ag Nps were performed using the ULTRA 55, Field Emission Scanning Electron Microscope (Karl Zeiss). The scanning was carried out using Inlens secondary electron detector, the voltage was maintained at 5.0 kV, and the working distance was kept at ∼5 mm. The SEM micrographs were obtained at various magnifications. AFM analyses of the biosynthesized silver colloids were performed using Agilent 5500 series (Agilent Technologies Inc., USA). All the images presented are tapping mode height images, recorded using a tip of force constant 40 N/m. Zeta potential of the bio Ag Nps were measured using Brookhaven Zeta PALS analyzer. The bio Ag Nps were diluted (1:6) using Milli-Q water and 3 mL aliquots were taken in quartz cuvette for measurements.

Raman spectra were recorded using a Renishaw InVia Raman microscope with an Ar^+ ion laser with the excitation wavelength of 514.5 nm. The laser beam was set in position with a 50x long working distance objective lens with a numerical aperture of 0.5 mounted on a Leica upright microscope (Leica Microsystems CMS GbmH, Wetzlar, Germany). Peltier cooled charge coupled device (CCD) array detector (1024 × 256 pixels) was used to detect the signals from a 2400 grooves/mm grating spectrometer. The observed data were processed and analyzed using Origin 8.5 (Origin Lab Corporation, MA) software. The spectra were collected at a spectral resolution of ±1 cm^{-1}. The acquisition time was 25 s, the incident power used was 0.03 mW and the number of accumulations was two for conventional Raman and the SERS studies on Rh B. In the case of TNT, the normal Raman spectrum of 1 M TNT solution in acetonitrile was acquired for 10 s using 30 mW laser and 1 accumulation. The SERS spectra of TNT in clove (C) and pepper (P) Ag Nps were acquired for 10 s using 3 mW laser power and 5 accumulations. The normal Raman spectrum of millimolar concentration of CL-20 was collected at 30 mW laser power for 10 s and 2 accumulations. For the SERS measurements of CL-20, 3 mW laser power with 10 s acquisition and 4 accumulations were used.

Biosynthesis of Silver Nanoparticles. Silver nanoparticles (Ag Nps) were biosynthesized using previously reported methods using cloves and pepper as natural precursors.[29−31] Both cloves and pepper have eugenol as a component. Additionally, pepper also contains piperine. Eugenol can release two electrons at a time which can be taken up by $2Ag^+$, thereby propelling the reduction of $AgNO_3$.[29] Briefly, 1.25 g of cloves was soaked in 25 mL of Milli-Q water for 24 h. The extract was collected after filtration and was used for further experiments. Synthesis of bio Ag Nps was carried out by taking $AgNO_3$ as starting material. Then a 3.33 mM $AgNO_3$ solution was stirred at 300 rpm, and the temperature was maintained at 75 °C, to which measured amount of clove extract was added. $AgNO_3$ to clove extract ratio was varied from 1:1 to 1:0.01 and the best yield was obtained for 1:0.25 ratios. The reduction was complete in about 2h which was identified by the formation of greenish yellow color of cloves Ag Nps (C Ag Nps). The same protocol was carried out for the biosynthesis of pepper-reduced Ag colloids (P Ag Nps) except that 2.5 g of pepper was used to prepare the

dx.doi.org/10.1021/jp4090266 | J. Phys. Chem. A XXXX, XXX, XXX−XXX

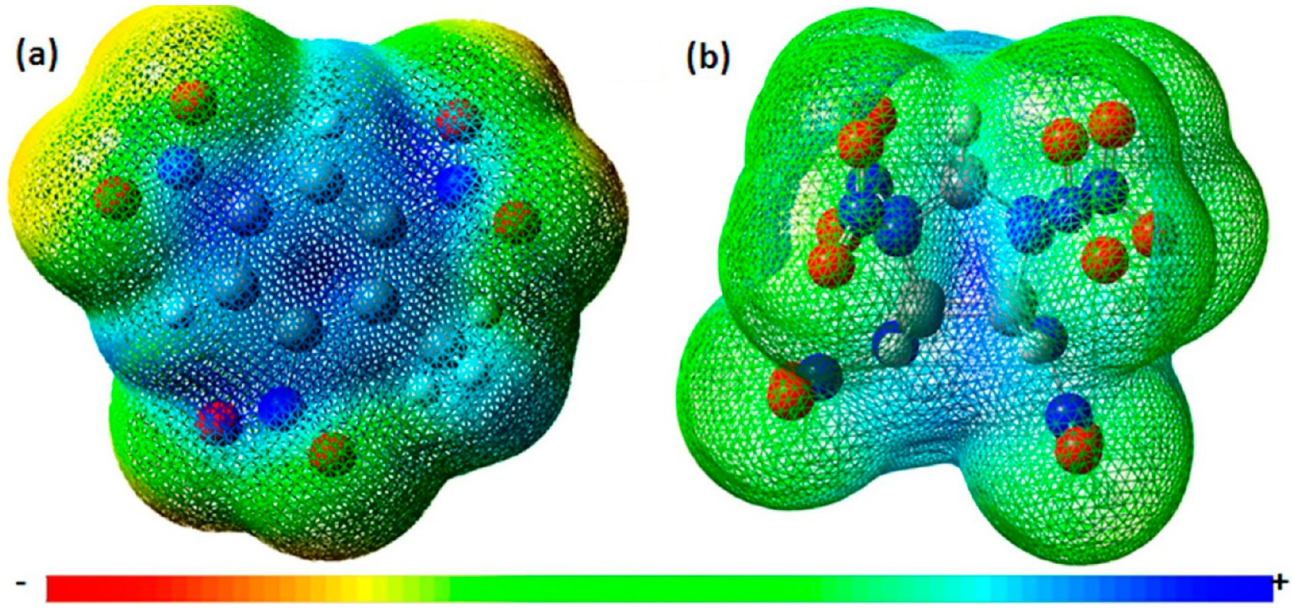

Figure 2. Molecular electrostatic potential mapped on the isodensity surface for (a) TNT in the range from −4.496e-2 (red) to +4.496e-2 (blue) and (b) CL-20 in the range from −8.530e-2 (red) to +8.530e-2 (blue) calculated at the B3LYP/6-311++G (d,p) level of theory, respectively.

extract. Hereafter we refer to silver nanoparticles obtained by the reduction of clove extract and pepper extract as C Ag Nps and P Ag Nps, respectively.

SERS Samples. The synthesized bio Ag Nps were washed in chloroform and water several times to remove any unreacted reducing agent or organic contaminant in the colloids. SERS samples were prepared by mixing equal amounts of freshly washed bio Ag Nps, 50 mM HCl, and the analyte. SERS studies on Rh B and TNT were conducted using the drop-casted sample on the aluminum slide. In the case of CL-20 SERS, samples were casted on the MgF_2 slides and air-dried before measurement. The samples were prepared before each experiment by diluting mM concentration of stock TNT and CL-20 solutions in acetonitrile. The final concentration of the analyte in the Ag Nps mixture was estimated to be 400 pM.

COMPUTATIONAL DETAILS

Molecular geometries of all the forms of TNT and CL-20 were optimized by DFT using 6-311++G (d, p) basis set and Becke's three parameter (local, nonlocal, and Hartree−Fock) hybrid exchange functionals with Lee−Yang−Parr correlational functional (B3LYP).[32−34] B3LYP has been demonstrated to be a suitable hybrid functional for the vibrational frequency calculations of both the ground and the lowest triplet state of organic molecules.[35−38] The vibrational frequency calculations were conducted at the same level for all the conformers to test the stability of their computed molecular structures. Positive values in all cases confirmed the stability of the minimum energy molecular structure. A complete vibrational assignment was also conducted for these compounds. For this purpose the vibrational frequencies in the harmonic approximation were calculated using software Gaussian 09[39] which provides weightage values of internal coordinates for vibrational assignments. Since the DFT derived vibrational frequencies are known to deviate from the experimental wavenumbers due to the neglect of anharmonicity effects, they are usually scaled down by the dual scaling procedure. Halls et al.[40] have made a critical analyses of experimentally measured and calculated wavenumbers at different levels of theory and divided the normal modes in the two regions. In the present study, the Raman spectra were acquired in the lower wavenumber (below 1800 cm^{-1}) region only; therefore, a scaling factor of 0.9927 was used for our calculations.

Potential energy distributions along the internal coordinates were calculated by software Gar2ped.[41] The graphical presentations of the calculated Raman spectra were made using Gauss View program.[42] By combining the results of the Gauss View program with symmetry considerations, vibrational mode assignments were made with a high degree of accuracy. The normal-mode analysis was performed, and the PED was calculated along the internal coordinates using localized symmetry.[43,44] For SERS calculations, the LANL2DZ basis set was used.

Molecular Electrostatic Potential. The molecular electrostatic surface potential (ESP) provides a charge density map, indicating the most probable interaction of a charged point-like species on organic molecules.[45−48] The electron density isosurface on to which the electrostatic potential surface was mapped has been provided in Figure 2, parts a and b, for TNT and CL-20 molecules, respectively.

The different values of the electrostatic potential at the surface are represented by different colors; the color varies from red to blue representing the regions of most negative electrostatic potential to the most positive electrostatic potential respectively and green represents regions of zero potential. Potential increases in the order of red < orange < yellow <green < blue.

In addition to ESP calculations, the Fukui function (FF)[49] was also calculated for the analyte molecules to obtain meaningful insight about the reactivity. FF provides a qualitative description about the reactivity of a molecule in terms of philicity. Hirshfeld atomic charges obtained from the DFT calculations employing the 6-31G(d,p) basis set was used for this purpose. FF was calculated for both TNT and CL-20 in neutral, cation and anion state of the molecules [for details see Table S1 and S2 of the Supporting Information].

To find the most favorable site for both TNT and CL-20 molecule for the attachment with Ag, the calculations had been

dx.doi.org/10.1021/jp4090266 | J. Phys. Chem. A XXXX, XXX, XXX−XXX

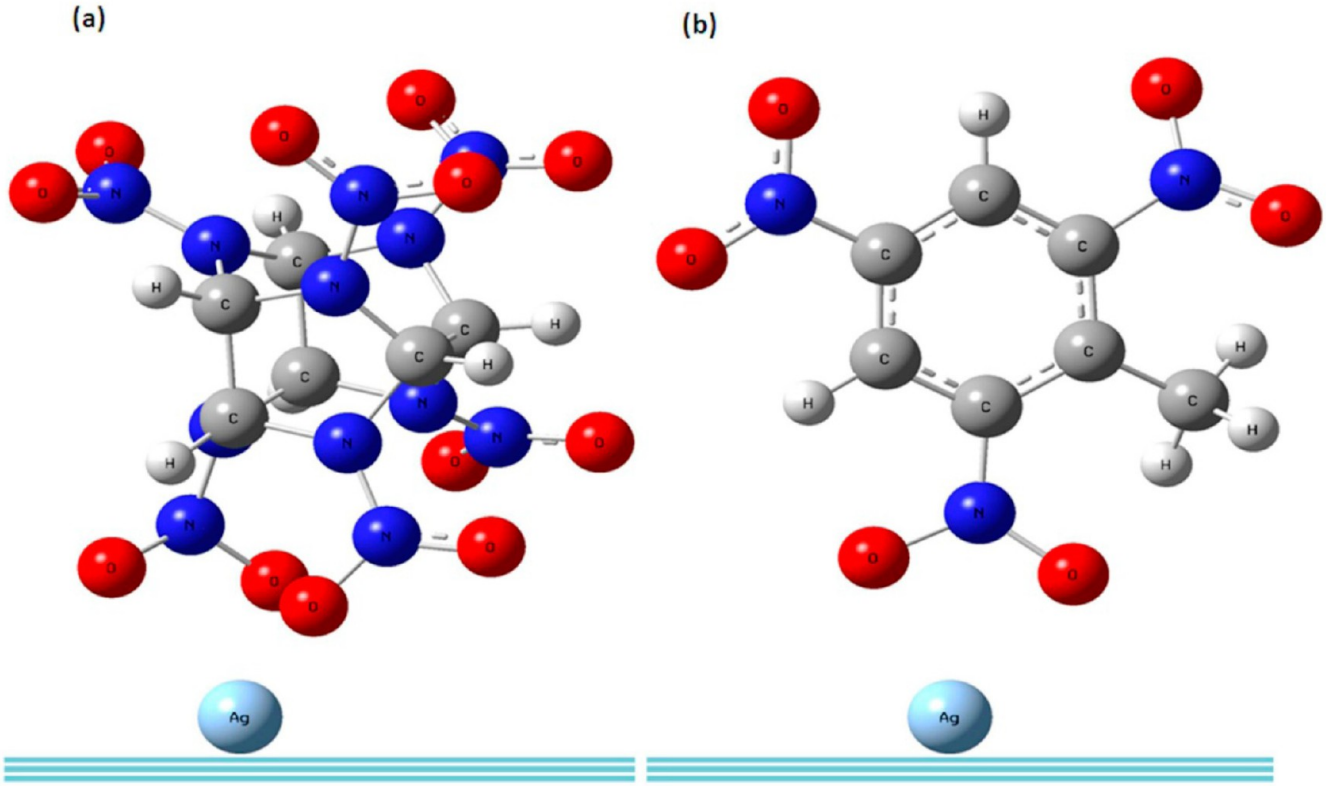

Figure 3. Optimized structure of (a) TNT and (b) CL-20 with silver atom.

carried out in all possible configurations and the most stable configuration has been reported here (Figure 3, parts a and b).

In the present study, only the most stable orientation which correlates well with the experimental results is presented.

RESULTS AND DISCUSSION

UV−vis absorption studies provide the optical response at the wavelength corresponding to localized surface plasmon resonances of the nanoparticles.[50] The experiments were carried out by diluting the silver colloids in the ratio 1:20 (Ag Nps: Milli-Q H_2O). Figure 4 shows the UV−vis spectra of the silver colloids synthesized using clove and pepper extract whose λ_{max} were at 545 and 467 nm, respectively.

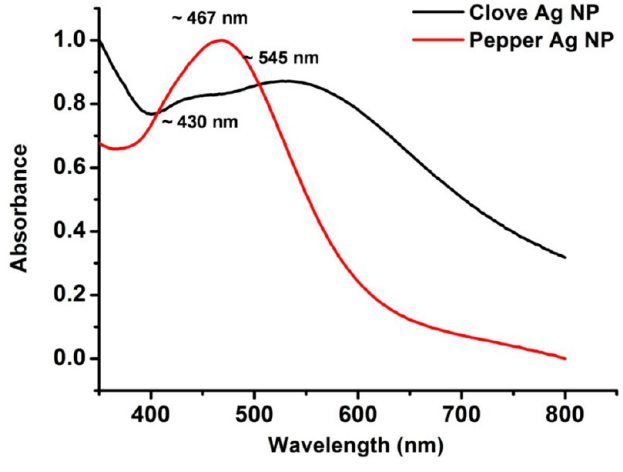

Figure 4. UV−vis spectra of biosynthesized silver nanoparticles using clove and pepper as reducing agent.

In addition, the C Ag NPs showed a small hump around 430 nm. The UV−vis spectra for C Ag Nps and P Ag Nps had difference in their appearance that was indicative of the morphological differences. The difference in λ_{max} values of C Ag Nps and P Ag Nps indicated that the P Ag Nps were smaller in size than C Ag Nps. The full-width half-maximum for C Ag Nps was almost twice than that of P Ag Nps which suggested that the polydispersity of C Ag Nps was greater than P Ag Nps.

The stability of colloids as a function of time was monitored using UV−vis to observe the change in the absorption maxima up to a period of 4 months in case of P Ag Nps and 5 months in case of C Ag Nps (Figure S3, parts a and b, Supporting Information). A significant decrease in intensity of λ_{max} was observed for C Ag Nps after 1 month and it remained almost constant thereafter until 5 months. However, in the case of P Ag Nps, the intensity of the absorbance maximum was the same even after 1 month which showed a gradual decrease after 4 months.

The morphologies of C and P Ag Nps were also observed from scanning electron microscopic (SEM) and atomic force microscopic (AFM) studies. The representative images are given in the Figures 5 and 6, respectively.

The micrographs clearly indicated that the synthesized colloids were polydisperse in nature and in aggregated state. The C Ag Nps were found to be more aggregated than the P Ag Nps and the extent of polydispersity was also more in the case of C Ag Nps. In addition, the particle shape was quasi-spherical in both the cases. The C Ag Nps were bigger in size (~90 nm) as compared to the P Ag Nps (~30 nm). These observations are consistent with the SEM studies. Surface charge plays an important role in colloidal chemistry as it affects the colloidal stability and also determines the extent of adsorption of analyte molecules onto the colloidal particles.

dx.doi.org/10.1021/jp4090266 | J. Phys. Chem. A XXXX, XXX, XXX−XXX

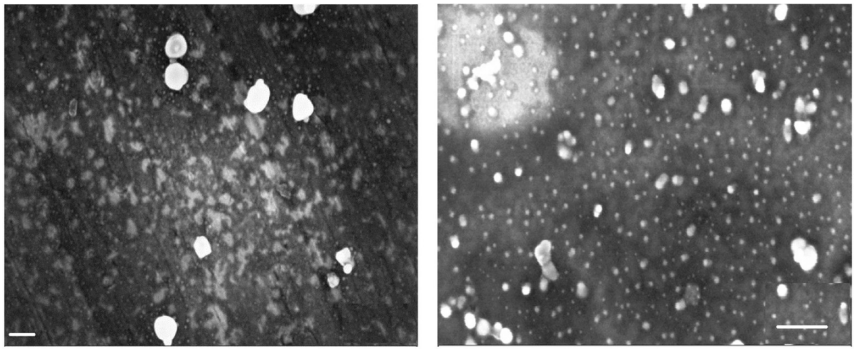

Figure 5. SEM micrograph of (a) clove Ag Nps at 159.57 × 10^3× magnification and (b) pepper Ag Nps at 277.65 × 10^3× magnification (scale bar = 100 nm).

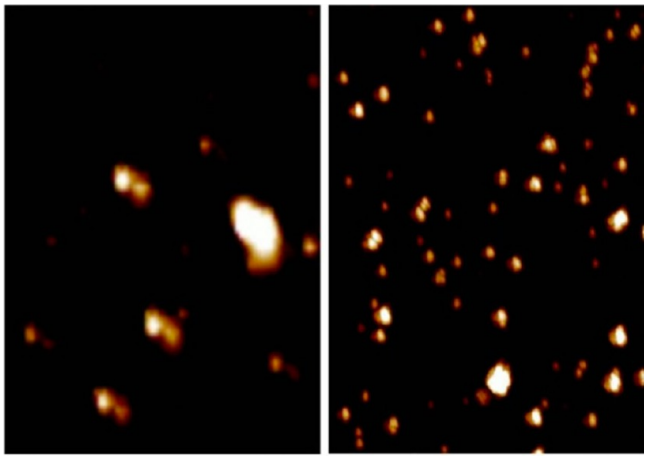

Figure 6. AFM image of (a) clove and (b) pepper Ag Nps (scale from 0.0 to 2.4 μm).

This in turn is a prerequisite for strong enhancement of Raman signals in SERS. The surface charge developed on C and P Ag Nps were measured using ζ potential, which refers to the potential at the interfacial double layer at a location of the slipping plane against a point in the solvent away from the interface.[51] Hence, ζ potential is an important parameter that provides useful information on the nanoparticle stability and its ability to interact with analyte molecules. High ζ values (negative or positive) indicate colloidal stability whereas low ζ values indicate instability due to partial aggregation and collapse of Ag Nps.[52] The ζ potential of clove Ag Nps was found to be −29.51 mV at a pH of 5.51 and that of pepper Ag Nps was −34.3 mV at a pH of 5.59. The ζ potential values obtained for bio Ag Nps revealed that the colloids showed moderate stability.

SERS Study on a Model Compound Rhodamine B. Xanthene based dyes, such as Rhodamine 6G (Rh 6G) and Rhodamine B (Rh B), have been widely used as model systems for understanding SERS as they show intense characteristic spectra and have been detected at single molecule level.[10,53] These dyes are strongly fluorescent which have molecular resonance Raman effect when excited into their visible absorption band. Surface enhanced resonance Raman spectros-

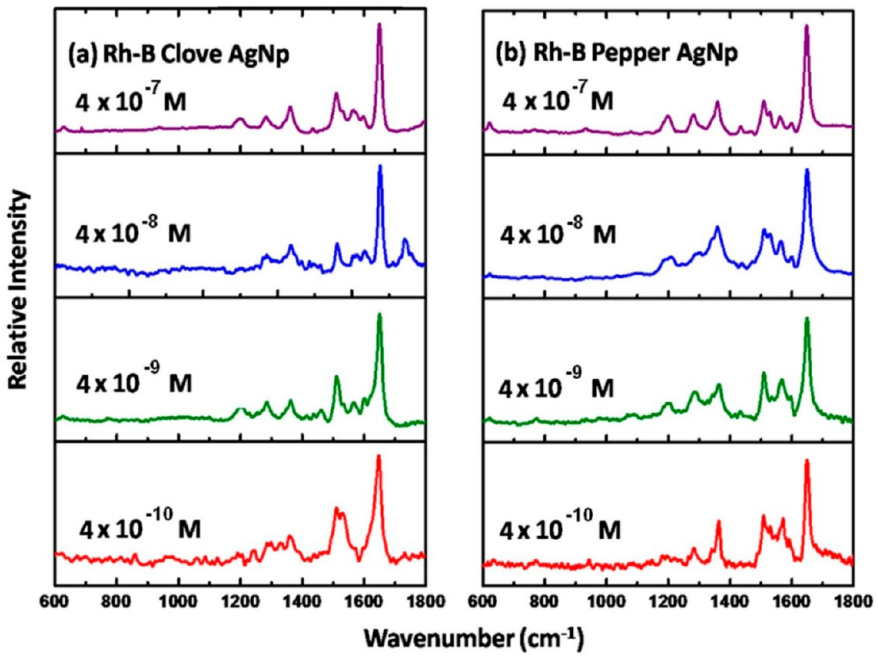

Figure 7. SERS Spectra of Rhodamine B at various concentrations using (a) clove and (b) pepper Ag Nps.

dx.doi.org/10.1021/jp4090266 | J. Phys. Chem. A XXXX, XXX, XXX−XXX

Table 1. Experimental and Computed Wavenumbers for TNT and Their Tentative Assignments[a]

Raman freq					SERS Raman freq			
					computational		experimental	
expt (solid)	unscaled values	scaled values	PED % (simplified description)	expt (1 M)	unscaled	scaled	clove	pepper
735	741	736	NO_2 def + ring def + NC str	–	735	730	748	734
793	806	800	NO_2 def + CC str ring	792	–	–	–	794, 810
823	848	842	NO_2 def + ring def	827	855	849	–	824, 856
908	917	910	NO_2 def + NC str + CC str.	939	910	903	896	904, 916
1088	1096	1088	CCH def + CC str + NC str	1083	1042, 1084	1034, 1076	1070, 1111	1006, 1077, 1101
1170	1180	1171	ring def + NC str + CC str + CCH def	1168	1139	1131	1147	1125, 1171
1212	1215	1206	CCH def + CCC def + CC str + CCN def	1208	1209, 1233	1200, 1224	1233	1205
1293	1344	1334	ring str	–	1264, 1313	1255, 1303	1284, 1313	1260, 1336, 1317
1359	1376	1366	NO_2 str + NO_2 def	1356	1375	1365	1370	1375
1438	1421	1411	ring str + CCH def	1438	1403, 1446	1393, 1435	1407, 1434	1425
1468	1474	1463	ring str + CCH def + CCN def + CH_3 def	1477	1490	1479	1461	1482
1532	1600	1588	NO_2 str + ring (str + def)	1544	1603	1591	1501, 1550, 1579	1525, 1551
1616	1622	1610	NO_2 str + CNO rocking	1616	1618	1606	1625	1622

[a]Note: All frequencies are in cm^{-1}. str: stretch, def: deformation.

Table 2. Experimental and Computed Wavenumbers for CL-20 and Their Tentative Assignments

Raman freq					SERS Raman freq			
					computational		experimental	
expt	unscaled values	scaled values	PED % (simplified description)	expt (1 mM)	unscaled	scaled	cloves	pepper
795	812	806	cage tor + NC tor + NO_2 def	794	811	805	799, 810	794
842, 903	847	841	NC tor + NO_2 def	842			838	839, 857
935, 960, 989	986	979	ring tor + NN (oop) + CC str	987	999	992	935, 1002	959, 989
1050	1043	1035	NC tor + ring tor + NCH def	1048	1041	1033	1053	1046
	1075	1067	ring tor + CH (oop) + NC str + NN str	–	1068	1060	1069	1061
1093	1104	1096	NC tor + NCH def + NN str	1091	1090	1082	1094	1092
1152	1190	1181	CH (oop) + NC tor + NCH def	–	1187	1178	1159, 1176	1148
1228	1215	1206	(NCH + ring) def	1227	1201	1192	1232	1228
1263	1262, 1278	1253, 1268	NCH def + NC tor + NO str + CC tor	1261	1248, 1265	1239, 1256	1267	1258
1297	1299, 1313	1290, 1303	CH (oop) + NCH def + NO str + NC tor	1293	–	–	1299	1297
1329	1356	1346	NO str + NCH def + CH (oop) + NO_2 def	1328	1340	1330	1332	1333
1384	1385	1375	CH (oop) + NCH def	1383	1406	1396	1391	1383
	1421	1411	CH (oop)	–	1439	1428	1420, 1451, 1495	1492
1626	1637	1625	NO_2 str + CNN def	1628	–	–	1558	1557
	1652	1640	NO_2 str	–	–	–	1589, 1633	1598, 1631

Note: All frequencies are in cm^{-1}. str: stretch. tor: torsion. oop: out of plane motion. def: deformation.

copy (SERRS) of Rhodamine 6G (Rh6G) has also been reported in the literature.[11,54−57] For this particular study, Rh B was chosen, which has a similar structure to Rh 6G with the exception of having two ethyl groups attached to nitrogen and having no methyl groups (Figure 1a). SERRS studies of Rh B on both C and P Ag Nps were conducted (Figure 7a and b) in the concentration range of 4×10^{-7} M to 400 pM concentration.

The SERRS peaks and corresponding assignments observed for Rh B on C and P Ag Nps agree well with the values reported in earlier literature.[53,55,58] For the case of 4×10^{-7} M Rh B solution, SERRS peaks at 621, 1198, 1282, 1360, 1510, 1560, and 1648 cm^{-1} were observed for both C and P Ag Nps which are shown in the Figure 7a and 7b, respectively. On the basis of earlier reports,[53,56,57] the peak at 621 cm^{-1} has been attributed to C−C−C ring in plane bending, and the peak at 1198 cm^{-1} could be due to aromatic C−H bending of the xanthene ring, in plane xanthene ring deformation and N−H bend. The peak at 1282 cm^{-1} could also be attributed to C−O−C stretch. The bands at 1360, 1510, and 1560 cm^{-1} have been assigned for aromatic C−C stretch, respectively. The strongest SERRS enhancement was observed at 1648 cm^{-1} which is due to the aromatic C−C stretching mode of xanthene ring. Interestingly, the 621 cm^{-1} peak for C−C−C ring in plane bending was not observed in any SERRS spectra at very low concentrations (10^{-8}−10^{-10} M). Similar peaks were observed for 4×10^{-8} and 4×10^{-9} M Rh B solution in both C and P Ag Nps, respectively. On further going down to 400 pM Rh B, the C Ag Nps SERRS peaks were observed at 1366, 1510, and 1647 cm^{-1} in case of P Ag Nps, SERRS of 400 pM Rh B were observed at 1284, 1364, 1510, 1555, and 1647 cm^{-1}.

dx.doi.org/10.1021/jp4090266 | J. Phys. Chem. A XXXX, XXX, XXX−XXX

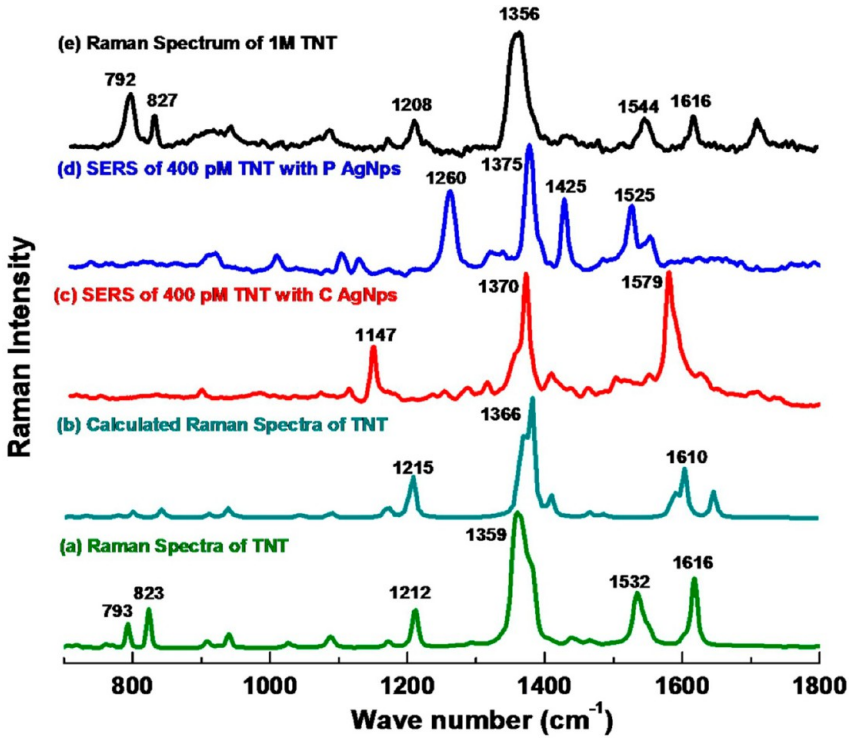

Figure 8. (a) Experimental Raman scattering spectra of TNT in the region 700−1800 cm^{-1}, (b) calculated (scaled), (c) 400 pM of TNT on C Ag NPs, and (d) 400 pM of TNT on P Ag NPs and (e) Raman spectra of 1 M TNT in ACN.

SERS Study on Explosives. After having obtained the SERS signals for Rh B with C and P Ag Nps at picomolar concentration levels successfully, SERS studies on two classes of military explosive molecules viz. nitro-aromatic (TNT) and nitramine (CL-20) were conducted. In order to substantiate the experimental observations, computational studies were also carried out for the normal Raman and SERS for both the explosive molecules (TNT and CL-20). The molecular orientation and site preference of the analyte molecule on the surface of Ag Nps can be gleaned from the ESP and FF calculations. ESP were plotted for both the molecules [details have been provided in the Computational Details section], which indicated the most preferred binding sites for the analytes on to the Ag surface. Therefore, with this prefound site model, the structure and vibrational frequencies were computed, which are presented in Table 1 and 2.

SERS Study on TNT. The normal Raman spectrum recorded for the solid TNT along with the computational result is shown in Figure 8, parts a and b. Raman bands of TNT were found to be in agreement with Raman spectra of this molecule reported previously.[59,60] The TNT molecule can be unequivocally identified by the symmetric and the asymmetric NO_2 stretching vibrations, observed at 1359 cm^{-1} and at 1532 and 1616 cm^{-1}, respectively. The other peaks can be assigned to the NO_2 deformation modes (793, 823 cm^{-1}), and the CCH (ring) bending modes (800−1200 cm^{-1}) and to the ring-breathing at 1212 cm^{-1}.[59] Before proceeding with the SERS studies on the explosive molecules, the blank spectra of C and P Ag Nps with acetonitrile and the activating agent HCl were recorded and have been provided in the Supporting Information, Figure S4, parts a and b. By following the protocol previously mentioned for SERRS of Rh B, SERS of TNT was recorded for 400 pM concentrations of TNT in solution using both C and P reduced Ag Nps respectively (Figure 8, parts c and d). It was observed that the NO_2 stretching vibrations, both symmetric as well as asymmetric were greatly enhanced. In the SERS spectra of TNT in C and P reduced Ag Nps, the strongest peaks were observed in between 1100 and 1600 cm^{-1}. The SERS spectra of TNT on C and P Ag Nps were different from the normal Raman spectra of TNT. Peaks were shifted and there were appearance of new peaks.

In the case of a 400 pM concentration of TNT, the SERS peaks which were characteristically pronounced were centered at 1147, 1370, and 1579 cm^{-1} bands for C Ag Nps and at 1260, 1375, 1425, 1525, and 1551 cm^{-1} bands respectively for P Ag NPs and has been shown in Figure 8, parts c and d [Table 1]. The probable mode assignments of the peaks were made based on the potential energy distribution (PED) analysis using Gar2PED software package (details have been provided in the Computational Details section). In case of C Ag Nps, the 1147 cm^{-1} peak mainly corresponds to a mixed mode comprising of ring deformation, NC and CC stretching modes, whereas the 1370 and 1579 cm^{-1} peaks could be attributed to symmetric and asymmetric NO_2 stretching modes. Additionally, there were appearances of some new peaks around 1111, 1313, 1407, 1501, and 1579 cm^{-1} respectively, which were not present in normal Raman spectra of TNT. Peaks observed at 1111, 1313, and 1407 cm^{-1} were assigned to ring stretching mode and the peaks at 1501 and 1579 cm^{-1} could be assigned to asymmetric nitro-stretching modes.

However, in the case of P Ag NPs, bands at 1260 and 1425 cm^{-1} were observed which could be attributed to ring stretching and CCH deformation modes based on the computational calculations. Peaks centered at 1375, 1525, and 1551 cm^{-1} were assigned mainly to symmetric and asymmetric nitro stretching modes. The 1260 and 1551 cm^{-1} bands were not observed in normal Raman spectrum of TNT. Additional peaks were also observed around 1006, 1125 cm^{-1} in case of

dx.doi.org/10.1021/jp4090266 | J. Phys. Chem. A XXXX, XXX, XXX−XXX

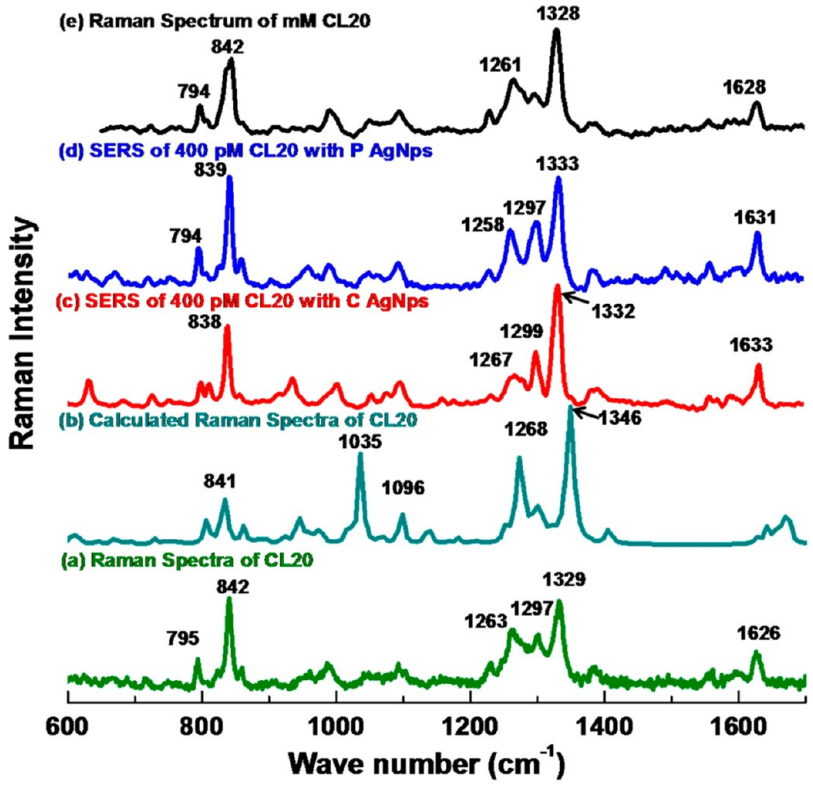

Figure 9. (a) Experimental Raman scattering spectra of CL-20 in the region, 600−1700 cm^{-1}, (b) calculated (scaled), (c) 400 pM of CL-20 on C Ag NPs, and (d) 400 pM of CL-20 on P Ag NPs and (e) Raman spectra of 1 mM CL-20 in ACN.

SERS of TNT on P Ag Nps. These peaks could be assigned to CCH deformation, ring deformation, stretching of NC and CC modes, respectively. Detailed assignments are given in Table 1. Knipp et al.[18] and Fierro-Mercado et al.[61] have already reported about the observation of peak shifts and appearance of new peaks in case of SERS of TNT on gold and silver substrates. On the basis of their observation they concluded that the TNT molecules lie flat on the Ag colloids and perpendicular on gold colloids. Selective enhancement of the vibrational bands of TNT in C Ag NPs and P Ag NPs may occur as a result of the interaction and orientation of TNT with the nanoparticles: in particular, the presence of three electron withdrawing $NO_2(-\delta)$ moieties cause the phenyl ring to develop a slight positive charge $(+\delta)$. In addition, due to the presence of the CH_3 moiety, the NO_2 groups present in the 2 and 6 positions are sterically hindered which results in these groups to deviate from planarity with respect to the phenyl ring. Furthermore, there could be reduction in the molecular symmetry of the molecule when it gets adsorbed on to the silver substrate. These surface interactions may lead to appearance of new bands which are absent in the normal Raman spectra of the molecule. In addition, the Ag Nps have different surface charges and state of aggregation as seen through the ζ potential measurements and SEM studies, these provide different environment for the analyte and hence, lead to differences in the interaction in the molecule for different Ag NPs. In the case of TNT SERS on C Ag NPs and P Ag NPs, the NO_2 modes are particularly enhanced. As reported in the literature, enhanced Raman signals are observed only for those vibrational modes that are in the close proximity of the surface plasmons of the Ag NPs.[18,61,62] Hence, the appearances of peaks as well as their intensities are affected by the extent of interaction of the analyte molecule with the silver nanoparticle. Similar observation has been reported in the literature for other molecules.[5] On the basis of the ESP plot along with the Fukui functions using Hirshfeld atomic charges for TNT, it was observed that the nitro group at the para position had maximum positive value for f_k^- (For details see Table S1 of Supporting Information) which indicated that this site could interact with Lewis bases. From the above discussion it can be suggested that the interaction of TNT with the Ag colloids happen via the NO_2 groups. This can be achieved by a perpendicular orientation of the TNT molecule on the Ag surface. In addition, the SERS peaks obtained for the CCH in plane bending modes in TNT could be indicative of a perpendicular orientation of TNT on to Ag surface.[61] It is known[5,63] that the vibrational modes of chromophore groups that are attached perpendicular to the surface of the metal are enhanced more whereas the modes with parallel polarizability components with respect to the surface will not be enhanced as reflected in the obtained SERS spectra. Currently, further studies are being carried out extensively to develop a deeper understanding of the interaction of TNT on Au and Ag colloids to prepare molecule specific sensors.

SERS Study on CL-20. The normal Raman spectrum recorded for the solid CL-20 along with the computational result is shown in Figure 9 a and b. Raman bands of CL-20 were found to be in agreement with Raman spectra of this molecule reported previously.[27,28]

For the SERS studies of CL-20 on C and P Ag Nps, the $CHCl_3$ washed colloids, activating agent (mM HCl) along with the analyte were mixed thoroughly and the drop was casted on the MgF_2 substrate which was allowed to dry before probing. All the spectra were collected from 600−1700 cm^{-1} to cover most of the Raman bands of CL-20. Figure 9c−e shows the SERS spectra of CL-20 in C Ag Nps and P Ag Nps as well as

dx.doi.org/10.1021/jp4090266 | J. Phys. Chem. A XXXX, XXX, XXX−XXX

conventional Raman spectra of mM dried CL-20 molecule, respectively. In the SERS spectra of CL-20 in C and P reduced Ag Nps, the strongest peaks were observed in the range 790−1630 cm^{-1}. In the case of 400 pM concentration, the peaks which were characteristically pronounced were centered at 799, 810, 838, 935, 1002, 1053, 1069, 1094, 1232, 1267, 1299, 1332, 1391,1495, 1558, 1589, and 1633 cm^{-1} for C Ag Nps and 794, 839, 857, 959, 989, 1046, 1061, 1092, 1148, 1228, 1258, 1297, 1333, 1383, 1492, 1557, 1598, and 1631 cm^{-1} for P Ag Nps respectively [Table 2].

On the basis of the PED analysis of the calculated normal Raman spectra of CL-20 molecule, the assignments of the normal modes for the SERS peaks of CL-20 were made. The intense peaks which were centered at 838, 1267 (1258 for P Ag Nps), 1299 (1297 for P Ag Nps), 1332 and 1633 (1631 for P Ag Nps) cm^{-1} could possibly arise from the NO_2 deformation mode, symmetric and asymmetric stretching of the NO_2 group respectively [Table 2]. There were, however, contributions from NCH deformation and CH out of plane motions as well. The peak at 1053 cm^{-1} for C Ag Nps and 1046 cm^{-1} for P Ag Nps could be observed due to the ring torsion coupled with NCH bending modes. The 1069 cm^{-1} peak for C Ag Nps (1061 cm^{-1} for P Ag Nps) could be attributed to NN stretch, ring torsion and CH out of plane motion, respectively. Another mixed mode observed at 1094 cm^{-1} for C Ag Nps (1092 cm^{-1} for P Ag Nps) could be attributed to the contributions from NC torsion, NCH deformation and NN stretch, respectively. 1232 and 1228 cm^{-1} peak for C and P Ag Nps was assigned to NCH and ring deformation, respectively.[27] Detailed assignments are given in Table 2.

On the basis of the comparison of the SERS peaks of CL-20 and normal Raman peaks of solid CL-20 along with the computational results (Table 2), it was observed that the SERS signals correlate well with the signal from the solid state. It was also noted that the SERS spectra for CL-20 on both C and P Ag Nps were very similar to the normal Raman spectra of CL-20. This implies that the interaction between colloidal silver and CL-20 is weak and the CL-20 adsorption does not lead to strong changes in the molecular structure of the analyte.[18] The SERS spectra display many Raman bands strongly related to the spectrum of the "free" or bulk CL-20 molecule. It is interesting to note that, the weak interaction of CL-20 with the Ag surface is also reflected from the ESP plot that shows a neutral character (green in color) of the caged nitramine. The Fukui function calculated using Hirshfeld atomic charge for CL-20 molecule indicated that the nitro groups where maximum charge localization occurred showed high f_k^- values (For details see Table S2 of Supporting Information)

Lewis et al.[59] as early as 1997 have reported that the peaks lying between 1320−1370 cm^{-1} and 1530−1660 cm^{-1} are characteristic of nitroaromatic, nitramine, and nitrate ester explosives corresponding to symmetric and asymmetric stretches of nitro bands. These peaks can be used as identifiers for the detection of explosives. In the present study, for SERS of TNT, the characteristic marker peaks were observed at 1370 cm^{-1} (1375 cm^{-1} for P Ag Nps) and 1625 cm^{-1} (1551 cm^{-1} for P Ag Nps), and for SERS of CL-20, they occurred at 1332 and 1633 cm^{-1} (1631 cm^{-1} for P Ag Nps) for C Ag Nps, respectively.

As an approach to quantify the SERS signal, the enhancement factors (EF) for TNT and CL-20 molecules were calculated by analytical method.[64−67] Etchegoin et al.[68] had reported a comparative study of various enhancements factors, from which analytical enhancement factor method to evaluate EF had been adopted. A concentration (C_{RS}) of the analyte solution which produced a measurable Raman signal with intensity (I_{RS}) under normal Raman measurements was taken. In this case, a drop of 1 M solution of TNT in acetonitrile and 1 mM solution of CL-20 in acetonitrile were casted on the MgF_2 slide for obtaining Raman signals (Raman spectra for CL-20 was obtained in dried state) respectively. Keeping the experimental conditions the same, i.e., laser wavelength, power, objective and other spectrometer conditions, SERS measurements for the analytes, i.e., TNT and CL-20 at 400 pM concentration (C_{SERS}) were carried out which produced signals with intensity I_{SERS} . The analytical enhancement factors (AEF) were thus calculated using the following equation.[68]

$$\mathrm{AEF} = \frac{I_{SERS}/C_{SERS}}{I_{RS}/C_{RS}} \quad (1)$$

The calculated AEF for CL-20 with respect to 1332 cm^{-1} peak was $(5825/4 \times 10^{-10}\ \mathrm{M})(10^{-3}\ \mathrm{M}/1433) = 10.26 \times 10^7$ for C Ag Nps and 1333 cm^{-1} peak was $(1453/4 \times 10^{-10}\ \mathrm{M})(10^{-3}\ \mathrm{M}/1433) = 0.25 \times 10^7$ for P Ag Nps. The estimated AEF was $\sim 10^7$ in case of CL-20 for both colloids. Similarly, in the case of TNT, for the 1370 cm^{-1} peak for C Ag Nps and the 1375 cm^{-1} peak for P Ag Nps, the AEF was calculated to be $\sim 10^9$.

From the observed SERS results together with the AEF calculations, it can be inferred that the TNT molecule interacts with the Ag surface chemically which leads to peak shifts and appearance of new peaks. These observations are also suggestive of the fact that there could be a possible change in the molecular symmetry of TNT when it gets adsorbed on the Ag colloids. In the case of CL-20 molecules, however, the SERS spectra appeared to be similar to that of the normal Raman spectra of the molecule suggesting that the CL-20 molecule has relatively weaker interactions with Ag surface compared to TNT which is also manifested in the AEF calculations. This observation was also substantiated by the Raman activity values obtained through DFT calculations. The Raman activity value calculated for 1366 cm^{-1} mode for the TNT molecule was ~81.53 $Å^4$/AMU and that for the 1346 cm^{-1} mode for the CL-20 molecule was ~52.06 $Å^4$/AMU. These values indicate that the TNT molecule is more polarizable as compared to the caged nitramine, CL-20 molecule. However, a word of caution is necessary here, although the calculated AEF is a simple way of calculating relative enhancement and thus provides a probable estimate of the approximate enhancement. For a precise indicator for the enhancement factor, one has to take into consideration, various other parameters such as the substrate, plasmon intensity, analyte, and excitation wavelength *etc.* for the evaluation of the EF and other methods for calculating EFs are also available in the literature.[68]

■ CONCLUSIONS

In this work we have demonstrated SERS of high energy materials, TNT and CL-20, at 400 pM concentrations using biosynthesized Ag Nps from clove and pepper. The following points have emerged out from this study: (a) Raman enhancement could be observed for both TNT and CL-20 molecules. (b) TNT interacted with the silver surface strongly giving rise to peak shifts and appearance of new peaks. However, in the SERS spectra of CL-20, significant peak shifts were not observed and the SERS spectral profile appeared very similar to that of the normal Raman spectrum of CL-20 in solid

dx.doi.org/10.1021/jp4090266 | J. Phys. Chem. A XXXX, XXX, XXX−XXX

state indicating that the interaction between colloidal silver and CL-20 were relatively weaker than TNT and enhancements of peaks of CL-20 were mainly due to electromagnetic origin which is akin with the obtained AEF values. c) Finally, we could identify markers in the SERS spectra of TNT and CL-20 which will be useful for the detection and identification of explosives. This is the first example, to the best of our knowledge, where SERS of CL-20 molecule at 400 pM level concentration has been detected. Our results were also corroborated with the computational results. Hence, biosynthesized Ag Nps using clove and pepper are good candidates for obtaining SERS signals for high energy materials like TNT and CL-20 and thus have the potential to be used as substrates for the detection of explosives.

■ ASSOCIATED CONTENT

Supporting Information

Details of the molecular electrostatic potential, Fukui functions, UV−vis spectra showing the stability of C and P Ag Nps with time, and blank spectra of C and P Ag Nps with the solvent and activating agent. This material is available free of charge via the Internet at http://pubs.acs.org.

■ AUTHOR INFORMATION

Corresponding Author

*(S.U.) Telephone: 91-80-22932595/23601234, Fax: 91-80-23601552/23600803. E-mail: umapathy@ipc.iisc.ernet.in or umapathy_india@yahoo.com.

Notes

The authors declare no competing financial interest.

■ ACKNOWLEDGMENTS

The authors gratefully acknowledge DST, Indian Institute of Science, Bangalore, India, and DRDO for the resources and funds. S.U. acknowledges the J. C. Bose fellowship from DST. D.C. would like to thank University Grant Commission—Dr. D. S. Kothari Postdoctoral Fellowship for the financial support.

■ REFERENCES

(1) Fleischmann, M.; Hendra, P. J.; McQuillan, A. J. Raman spectra of pyridine adsorbed at a silver electrode. *Chem. Phys. Lett.* **1974**, *26*, 163−166.

(2) Albrecht, M. G.; Creighton, J. A. Anomalously intense Raman spectra of pyridine at a silver electrode. *J. Am. Chem. Soc.* **1977**, *99*, 5215−5217.

(3) Jeanmaire, D. L.; Van Duyne, R P. Surface Raman Spectroelectrochemistry Part I. Heterocyclic, Aromatic, and Aliphatic Amines Adsorbed on the Anodized Silver Electrode. *J. Electroanal. Chem.* **1977**, *84*, 1−20.

(4) Kneipp, K.; Moskovits, M.; Kneipp, H. *Surface-Enhanced Raman Scattering: Physics and Applications*; Springer. Berlin, 2006.

(5) Moskovits, M. Surface −enhanced Spectroscopy. *Rev. Mod. Phys.* **1985**, *57*, 783−828.

(6) Campion, A.; Kambhampati, P. Surface Enhanced Raman Scattering. *Chem. Soc. Rev.* **1998**, *27*, 241−250.

(7) Sharma, B.; Frontiera, R. R.; Henry, A. I.; Ringe, E.; Van Duyne, R P. SERS: Materials, applications and the future. *Mater. Today* **2012**, *15*, 16−25.

(8) Cialla, D.; März, A.; Böhme, R.; Theil, F.; Weber, K.; Schmitt, M.; Popp, J. Surface-enhanced Raman spectroscopy (SERS): progress and trends. *Anal. Bioanal. Chem.* **2012**, *403*, 27−54.

(9) Kniepp, K.; Wang, Y.; Kniepp, H.; Perelman, L. T.; Itzkan, I.; Dasari, R. R.; Feld, M. Single Molecule Detection Using Surface-Enhanced Raman Scattering (SERS). *Phys. Rev. Lett.* **1997**, *78*, 1667−1670.

(10) Nie, S.; Emory, S. R. Probing single molecules and single nanoparticles using surface enhanced Raman spectroscopy. *Science* **1997**, *275*, 1102−1106.

(11) Dieringer, J. A.; Wustholz, K. L.; Masiello, D. J.; Camden, J. P.; Kleinman, S. L.; Schatz, G. C.; Van Duyne, R. P. Surface-Enhanced Raman Excitation Spectroscopy of a Single Rhodamine 6G Molecule. *J. Am. Chem. Soc.* **2009**, *131*, 849−854.

(12) Ru, L.; Etchegoin, P. G. Single-Molecule Surface-Enhanced Raman Spectroscopy. *Annu. Rev. Phys. Chem.* **2012**, *63*, 65−87.

(13) Weienbacher, N.; Lendl, B.; Frank, J.; Wanzenbock, H. D.; Mizaikoff, B.; Kellner, R. Continuous surface enhanced Raman spectroscopy for the detection of trace organic pollutants in aqueous systems. *J. Mol. Struct.* **1997**, *410−411*, 539−542.

(14) Zhang, X.; Young, M A.; Lyandres, O.; Van Duyne, R. P. Rapid detection of an anthrax biomarker by surface- enhanced Raman spectroscopy. *J. Am. Chem. Soc.* **2005**, *127*, 4484−4489.

(15) Schmuck, C.; Wich, P.; Küstner, B.; Kiefer, W.; Schlücker, S. Direct and Label-Free Detection of Solid-Phase-Bound Compounds by Using Surface-Enhanced Raman Scattering Microspectroscopy. *Angew. Chem., Int. Ed.* **2007**, *46*, 4786−4789.

(16) Schlücker, S. SERS Microscopy: Nanoparticle Probes and Biomedical Applications. *ChemPhysChem* **2009**, *10*, 1344−1354.

(17) Xie, W.; Schlücker, S. Medical applications of surface-enhanced Raman scattering. *Phys. Chem. Chem. Phys.* **2013**, *15*, 5329−5344.

(18) Kniepp, K.; Wang, Y.; Dasari, R. R.; Feld, M. S.; Gilbert, B. D.; Janni, J.; Steinfeld, J. I. Near-infrared surface-enhanced Raman scattering of trinitrotoluene on colloidal gold and silver. *Spectrochim. Acta* **1995**, *51*, 2171−2175.

(19) Hatab, N. A.; Eres, G.; Hatzinger, P. B.; Gu, B. Detection and analysis of cycotrimethylenenitramine (RDX) in environmental samples by surface-enhanced Raman spectroscopy. *J. Raman Spectrosc.* **2010**, *41*, 1131−1136.

(20) Botti, S.; Cantarini, L.; Palucci, A. Surface-enhanced Raman spectroscopy for trace-level detection of explosives. *J. Raman Spectrosc.* **2010**, *41*, 866−869.

(21) Fang, X.; Ahmad, S. R. Detection of explosive vapour using surface-enhanced Raman spectroscopy. *Appl. Phys. B: Laser Opt.* **2009**, *97*, 723−726.

(22) Demeritte, T.; Kanchanapally, R.; Fan, Z.; Singh, A. K.; Senapati, D.; Dubey, M.; Zakarb, E.; Ray, P. C. Highly efficient SERS substrate for direct detection of explosive TNT using popcorn-shaped gold nanoparticle-functionalized SWCNT hybrid. *Analyst* **2012**, *137*, 5041−5045.

(23) Piorek, B. D.; Lee, S. J.; Moskovits, M.; Meinhart, C. D. Free-Surface Microfluidics/Surface-Enhanced Raman Spectroscopy for Real-Time Trace Vapor Detection of Explosives. *Anal. Chem.* **2012**, *84*, 9700−9705.

(24) Talian, I.; Huebner, J. Separation followed by direct SERS detection of explosives on a novel black silicon multifunctional nanostructured surface prepared in a microfluidic channel. *J. Raman Spectrosc.* **2012**, *43*, 4237−4240.

(25) Botti, S.; Almaviva, S.; Cantarini, L.; Palucci, A.; Puiu, A.; Rufoloni, A. Trace level detection and identification of nitro-based explosives by surface-enhanced Raman spectroscopy. *J. Raman Spectrosc.* **2013**, *44*, 463−468.

(26) Nielsen, A. T.; Chafin, A. P.; Christian, S. L.; Moore, D. W.; Nadler, M. P.; Nissan, R. A.; Vanderah, D. J.; Gilardi, R. D.; George, C. F.; Flippen-Anderson, J. L. Synthesis of Polyazapolycyclic Caged Polynitramines. *Tetrahedron* **1998**, *54*, 11793−11812.

(27) Goede, P.; Latypov, N. V.; Östmark, H. Fourier Transform Raman Spectroscopy of the Four Crystallographic Phases of α, β, γ, and ε 2,4,6,8,10,12-Hexanitro-4,6,8,10,12 hexaazatetracyclo-[5.5.0.05,9.03,11] dodecane (HNIW, CL-20). *Propellants Explos. Pyrotech.* **2004**, *29* (4), 205−208.

(28) Kholod, Y.; Okovytyy, S.; Kuramshina, G.; Qasim, M.; Gorb, L.; Leszczynsk, J. An analysis of stable forms of CL-20: A DFT study of conformational transitions, infrared and Raman spectra. *J. Mol. Struct.* **2007**, *843*, 14−25.

(29) Singh, A. K.; Talat, M.; Singh, D. P.; Srivastava, O. N. Biosynthesis of gold and silver nanoparticles by natural precursor clove and their functionalization with amine group. *J. Nanopart. Res.* **2010**, *12*, 1667−1675.
(30) Vijayaraghavan, K.; Kamala Nalini, S. P.; Prakash, N. U.; Madhankumar, D. Biomimetic synthesis of silver nanoparticles by aqueous extract of Syzygium aromaticum. *Mater. Lett.* **2012**, *75*, 32−35.
(31) Shukla, V. K.; Singh, R. P.; Pandey, A. C. Black pepper assisted biomimetic synthesis of silver nanoparticles. *J. Alloys Comp.* **2010**, *507*, 13−16.
(32) Becke, A. D. A new mixing of Hartree-Fock and local density-functional theories. *J. Chem. Phys.* **1993**, *98*, 1372−1377.
(33) Lee, C.; Yang, W.; Parr, R. G. Development of the Colic-Salvetti correlation-energy formula into a functional of the electron density. *Phy. Rev. B* **1988**, *37*, 785−789.
(34) Parr, R. G.; Yang, W. *Density Functional Theory of Atoms and Molecules*; Oxford, NY, 1989.
(35) Mohandas, P.; Umapathy, S. Structure and vibrational spectra of photogenerated intermediates of p-Benzoquinone investigated by density functional calculations. *J. Phys. Chem. A* **1997**, *101*, 4449−4459.
(36) Biswas, N.; Umapathy, S. Density functional studies on the vibrational spectra and normal modes of trans and cis-azobenzene. *J. Phys. Chem. A* **1997**, *101*, 5555−5566.
(37) Balakrishnan, G.; Mohandas, P.; Umapathy, S. Time-resolved resonance Raman, Ab initio Hartree Fock and density functional studies on the transient states of perfluoro-p-benzoquinone. *J. Phys. Chem. A* **2001**, *105*, 7778−7789.
(38) Puranik, M.; Chandrasekhar, J.; Sneijders, J. G.; Umapathy, S. Time resolved resonance Raman and density functional studies on the ground state and short lived intermediates of tetrabromo-p-benzoquinone. *J. Phys. Chem. A* **2001**, *105*, 10562−10569.
(39) Gaussian 09, Revision A.1. Frisch, M. J.; Trucks, G. W.; Schlegel, H. B.; Scuseria, G. E.; Robb, M. A.; Cheeseman, J. R.; Scalmani, G.; Barone, V.; Mennucci, B.; Petersson, G. A. et al. Gaussian, Inc.: Wallingford, CT, 2009.
(40) Halls, M. D.; Velkovski, J.; Schlegel, H. B. Harmonic Frequency Scaling Factors for Hartree-Fock, S-VWN, B-LYP, B3-LYP, B3-PW91 and MP2 with the Sadlej pVTZ Electric Property Basis Set. *Theor. Chem. Acc.* **2001**, *105*, 413−421.
(41) Martin, J. M. L.; Van Alsenoy, C. *GAR2PED*; University of Antwerp: Antwerp, Belgium, 1995.
(42) Frisch, A.; Nielson, A. B.; Holder, A. J. *GAUSSVIEW User Manual*; Gaussian Inc.: Pittsburgh, PA, 2000.
(43) Pulay, P.; Fogarasi, G.; Pang, F.; Boggs, J. E. Systematic ab initio gradient calculation of molecular geometries, force constants and dipole moment derivatives. *J. Am. Chem. Soc.* **1979**, *101*, 2550−2560.
(44) Fogarasi, G.; Zhou, X.; Taylor, P. W.; Pulay, P. The calculation of ab initio molecular geometries: efficient natural internal coordinates and empirical correction by offset forces. *J. Am. Chem. Soc.* **1992**, *114*, 8191−8201.
(45) Chis, V.; Venter, M. M.; Leopold, N.; Cozar, O. Raman, surface-enhanced Raman scattering and DFT study of para-nitro-aniline. *Vibr. Spectosc.* **2008**, *48*, 210−214.
(46) Naray-Szabo, G.; Ferenczy, G. G. Molecular Electrostatics. *Chem. Rev.* **1995**, *95*, 829−847.
(47) Mircescu, N. E.; Varvescu, A.; Herman, K.; Chis, V.; Leopold, N. Surface-enhanced Raman and DFT study on zidovudine. *Spectroscopy* **2011**, *26*, 311−315.
(48) Politzer, P.; Truhlar, D. G. *Chemical Application of Atomic and Molecular Electrostatic Potentials*; Plenum: New York, 1981.
(49) De Proft, F.; Van Alsenoy, C.; Peeters, A.; Langenaeker, W.; Geerlings, P. Atomic charges, dipole moments, and Fukui functions using the Hirshfeld partitioning of the electron density. *J. Comput. Chem.* **2002**, *23*, 1198−1209.
(50) Le Ru, E. C.; Etchegoin, P. *Principles of surface enhanced Raman spectroscopy and related plasmonic studies effects* Elsevier: Amsterdam, 2009; pp 367−380.
(51) Hiemenz, P. C.; Rajagopalan, R. *Principles of Colloid and Surface Chemistry*; Marcel Dekker: New York, 1997; pp 534−571.
(52) Alvarez-Puebla, R. A.; Arceo, E.; Goulet, P. J.G.; Garrido, J. J.; Aroca, R. F. Role of Nanoparticle Surface Charge in Surface-Enhanced Raman Scattering. *J. Phys. Chem. B* **2005**, *109*, 3787−3792.
(53) Hildebrandt, P.; Stockburger, M. Surface-Enhanced Resonance Raman Spectroscopy of Rhodamine 6G Adsorbed on Colloidal Silver. *J. Phys. Chem.* **1984**, *88*, 5935−5944.
(54) Link, S.; El-Sayed, M. A. Shape and size dependence of radiative, non-radiative and photothermal properties of gold nanocrystals. *Int. Rev. Phys. Chem.* **2000**, *19* (3), 409−453.
(55) Geiman, I.; Leona, M.; Lombardi, J. R. Application of Raman Spectroscopy and Surface-Enhanced Raman Scattering to the Analysis of Synthetic Dyes Found in Ballpoint Pen Inks. *J. Forensic Sci.* **2009**, *54* (4), 947−952.
(56) Michaels, A. M.; Nirmal, M.; Brus, L. E. Surface Enhanced Raman Spectroscopy of Individual Rhodamine6G Molecules on Large Ag Nanocrystals. *J. Am. Chem. Soc.* **1999**, *121*, 9932−9939.
(57) Jensen, L.; Schatz, G. C. Resonance Raman Scattering of Rhodamine 6G as Calculated Using Time-Dependent Density Functional Theory. *J. Phy. Chem. Lett.* **2006**, *110*, 5973−5977.
(58) Zhang, J.; Li, X.; Sun, X.; Li, Y. Surface Enhanced Raman Scattering Effects of Silver Colloids with Different Shapes. *J. Phys. Chem. B* **2005**, *109*, 12544−12548.
(59) Lewis, I. R.; Daniel, N. W., Jr.; Griffiths, P. R. Interpretation of Raman Spectra of Nitro-Containing Explosive Materials. Part I: Group Frequency and Structural Class Membership. *Appl. Spectrosc.* **1997**, *51* (12), 1854−1867.
(60) Passingham, C.; Hendra, P. J.; Willis, H. A. The Raman spectra of some aromatic nitro compounds. *Spectrochim. Acta* **1991**, *47A* (9/10), 1235−1245.
(61) Fierro-Mercado, P. M.; Hernandez-Rivera, S. P. Highly Sensitive Filter Paper Substrate for SERS Trace Explosives Detection. *Int. J. Spectrosc* **2012**, 716527.
(62) Jerez-Rozo, J. I.; Primera-Pedrozo, O. M.; Barreto-Cabán, M. A.; Hernández- Rivera, S. P. Enhanced Raman Scattering of 2, 4, 6- TNT Using Metallic Colloids. *IEEE Sensors J.* **2008**, *8*, 974−982.
(63) Moskovits, M.; DiLella, D. P.; Maynard, K. J. Surface Raman Spectroscopy of a Number of Cyclic and Molecular Reorientation Aromatic Molecules Adsorbed on Silver: Selection Rules. *Langmuir* **1988**, *4*, 67−76.
(64) Etchegoin, P. G.; Galloway, C.; Le Ru, E. C. Polarization-dependent effects in surface-enhanced Raman scattering (SERS). *Phys. Chem. Chem. Phys.* **2006**, *8*, 2624−2628.
(65) Zhao, J.; Jensen, L.; Sung, J.; Zou, S.; Schatz, G. C.; Van Duyne, R. P. Interaction of Plasmon and Molecular Resonances for Rhodamine 6G Adsorbed on Silver Nanoparticles. *J. Am. Chem. Soc.* **2007**, *129*, 7647−7656.
(66) Moskovits, M.; DiLella, D. P.; Maynard, K. J. Surface Raman Spectroscopy of a Number of Cyclic and Molecular Reorientation Aromatic Molecules Adsorbed on Silver: Selection Rules. *Langmuir* **1988**, *4*, 67−76.
(67) McFarland, A. D.; Young, M. A.; Dieringer, J. A.; Van Duyne, R. P. Wavelength-Scanned Surface-Enhanced Raman Excitation Spectroscopy. *J. Phys. Chem. B* **2005**, *109*, 11279−11285.
(68) Le Ru, E. C.; Blackie, E.; Meyer, M.; Etchegoin, P. G. Surface Enhanced Raman Scattering Enhancement Factors: A Comprehensive Study. *J. Phys. Chem. C* **2007**, *111*, 13794−1380.